ICE FORCES AGAINST ARCTIC OFFSHORE STRUCTURES

by
W. M. Sackinger
J. B. Johnson

FINAL REPORT
March 1, 1984
Contract No. DACA-89-83-K-0004
(Final Report Contract No. DACA-89-82-K-0001)

Submitted To

US Army Cold Regions Research and Engineering Laboratory
72 Lyme Road
Hanover, New Hampshire 03755

and to

US Department of the Interior
Minerals Management Service
MMS MS 620
12203 Sunrise Valley Drive
Reston, Virginia 22091

Geophysical Institute
University of Alaska
Fairbanks, Alaska 99701

I. BACKGROUND

This research program was initiated on December 1, 1981 with the objective of determining lateral forces on artificial islands and offshore structures which are subjected to moving sea ice. This was particularly oriented towards the exploration and development of Arctic oil and gas deposits in the Beaufort, Chukchi, and Bering Seas. The National Petroleum Council report of 1981 estimated that there is a risked mean value of 30.8 billion barrels of oil equivalent to be found in these ice-infested Alaskan offshore regions, encompassing approximately 262 million acres. Origination of the support for this work was with the U.S. Department of Interior, Minerals Management Service, and technical monitoring and contracting of the work was conducted by the US Army Cold Regions Research and Engineering Laboratory. Contract No. DACA89-82-K-0001 spanned the first year of effort on this research subject, and continuation Contract No. DACA89-83-K-0004 spanned the second year of research effort on this subject. This final report should be considered as a report of activities on both of the linked contracts, and should serve as final report for both contracts.

The approach which was taken in the research study reported here was to measure the ice stress at relatively large distances from offshore islands, to measure the ice lateral displacement simultaneously, and from the effective island width during ridgebuilding events (which represent intervals of high lateral force on the island structure) the total force on the offshore island or structure was to be calculated using an integration technique. Information obtained from this study was intended to be applied in the process of certification of

proposed designs for Arctic offshore islands and drilling structures, under the Minerals Management Service mandate for application of best available and safest technology.

The earliest offshore oil platforms in Cook Inlet, Alaska, were designed to withstand a pressure of 2070 kPa (300 psi) from the forces of moving sea ice. Instrumented structures in Cook Inlet have been subject to loadings of up to 1030 kPa (150 psi). An instrumented lighthouse in the Gulf of Bothnia has detected local ice pressures of as high as 2500 kPa (363 psi), but at the inception of this study there were no instrumented artificial structures available in the Alaskan Beaufort Sea which could be used to determine effective ice pressures at the boundary of the structures. At the inception of this program, a review of the strength of annual and multi-year ice was conducted, and the accepted technical practices for calculation of total ice force on an offshore structure were also reviewed. A review was also conducted of the measurements which had been made during the interval 1976-1981 of stresses in sea ice near artificial islands and natural islands.

As was pointed out in the first quarterly report, instrumentation of the ice sheet leads to a sequence of local readings of ice stress which can be affected by local variations in stress concentration due to cracks in the ice sheet or the irregularities in the boundary of the island or fixed structure. In order to avoid this type of problem, the experimental approach taken in this research program involved instrumenting the ice sheet at a distance several diameters away from the island, so that a fewer number of ice stress sensors could be used and a reasonably continuous distribution of ice stress could be expected. Ice stresses at greater distances from an island are expected

to be quite low, far below the failure stress, since failure obviously occurs at the island boundary first. However, the average stress at large distances from the island does translate into the total force upon the island by means of the complex transfer of stresses through the cracked and nonuniform ice rubble near the island. Deployment of sensors at great distances from an island involves either very long signal cables or telemetry links; the telemetry approach was employed in the research study which was undertaken.

The instrumentation which was designed for this study was to measure the ice stress, the ice sheet movement, together with the environmental conditions of windspeed and direction. A detailed discussion of the instrumentation can be found in the First Quarterly Report (Ref. 1). The uniaxial stress sensor, which was chosen for use in this study, is a stiff sensor which produces a stress concentration factor and which has a transverse sensitivity when embedded in the ice sheet. A discussion of the theory needed to interpret results from such a uniaxial stress sensor array was presented in detail in the Second Quarterly Report (Ref. 2). Also in the Second Quarterly Report is a discussion of the theory required for the interpretation of the results from a new ring strain gauge, which was introduced into the experimental program in order to provide for greater sensitivity, and to try to develop a localized relation of stress versus strain in 3 dimensions, for the sea ice at the site of the gauge installation.

The time allowed for fabrication of the experimental system, beginning with the inception of the contract on December 1, 1981, was not adequate to permit installation during winter 1981-82, so that installation was deferred until winter 1982-83. The additional time

available made it possible to consider several options for ice movement detection, including ranging systems which use fixed points of land as references, as well as bottom-reference systems using anchor cables. It was finally decided in 1982 to construct a bottom-reference ice positioning system, inasmuch as the expected movement of ice in the vicinity of an artificial island was expected to be small. Although attempts were to be made to measure ice stresses in active zones, it was not possible to arrange for such experimental activity in the Canadian Beaufort Sea adjacent to the Dome Petroleum Company Single Steel Drilling Caisson (SSDC), and so the winter 1982-83 installation was done in the vicinity of Shell Oil Company's Seal Island just northwest of Prudhoe Bay, Alaska.

During the 1982 interval, a paper was presented by Dr. J. B. Johnson entitled, "A Surface Integral Method for Calculating Ice Loads on Offshore Structures from In-Situ Measurements", (Ref. 3), which is presented as Appendix 1 of the Third Quarterly Report, (Ref. 4). During the interval September to December 1982, a considerable amount of electronic development effort was devoted to the construction and test of a ice movement system, including a direct digitally-modulated transmission signal derived from the shaft of the digital shaft encoder. The adaptation of a computer data acquisition system formerly used for seismic measurements was also a major effort during the fourth quarter, as described in the Fourth Quarterly Report, (Ref. 5).

As described in the research continuation proposal of November 1982, it was intended that ice stress and ice movement measurements would be made around an artificial island in the Beaufort Sea during winter 1982-83. It would have been optimum if the ice stress

measurement system could have been installed in a location where considerable ice activity was taking place early in the winter 1982-83. Arrangements were sought with Dome Petroleum Ltd. of Calgary, Alberta, to install the instrumentation in the vicinity of the Single Steel Drilling Caisson (SSDC) during winter 1982-83. Permission was not obtained from Dome Petroleum management to make this installation, and this alternative therefore was ruled out in January 1983. The option of making the installation in the vicinity of the Shell Oil Company's Seal Island just northwest of Prudhoe Bay, Alaska, was continually under serious consideration, and it was therefore obvious in February 1983 that the installation at the Shell Oil Company Seal Island represented the only viable alternative. (The Gulf Oil Canada caisson-retained island Tarsuit was instrumented during this period under the terms of a joint industry proprietary project and was possibly available as well, but practical difficulties of obtaining concensus permission plus logistics of deployment both weighed against this option at that time).

After a three month operational gap between contracts, the Contract No. DACA89-83-K-0004 was initiated on March 1, 1983, and deployment at Seal Island took place on March 5, 1983. The installation was completed by March 11, 1983 as described in detail in the Fifth Quarterly Report (Ref. 6). As is described in detail in Reference 6, the ice ridging which had taken place early in the winter was concentrated on the northwest side of Seal Island, with smaller, more widely distributed ice ridges prevalent on the northeast side. Inasmuch as the dominant direction of the winds for the interval March through May for this region of the North Slope come from the northeast and east, it was felt that the most likely direction for ice movement would be from the

northeast corresponding to the average movement of ice in the Beaufort Gyre. Hence the decision was taken to locate the array of instruments on the northeast side of Seal Island. Three separate stations were deployed, as shown in Figure 1. The central station, Site S3, was located 570 m from the center of Seal Island. The central station contained three uniaxial stress sensors oriented in a rosette, as well as nine strain sensors and a two-channel ice movement station. Stations S1 and S2 each contained three stress sensors in a rosette. The ice sheet thickness was 180 cm and the water depth was 10.16 m at site S3. From the small freeboard of the light ice ridges surrounding all three stations, it was obvious that the ice sheet was definitely not grounded in the vicinity of the installation. It was therefore felt that a significant wind from the northeast would result in additional ice ridging at the boundary of the rubble near the island, and that there was a high probability of recording the ice stress distribution during such a severe weather event. All data was telemetered back to the island, where it was digitized and recorded on magnetic tape for subsequent analysis.

As indicated in the Fifth Quarterly Report, the ice salinity profiles ranged from 8 to 12 $^{o}/oo$ at the surface to about 4 $^{o}/oo$ at the 90 cm depth. This is typical of annual ice which has formed by freezing in place throughout the winter season. Duration of the experimental period was 50 days, from March 11 to April 30, 1983. Although it was originally intended to attempt to maintain the system for a longer interval in May, it was not possible to do so because of the abnormally warm weather which was causing a rapid deterioration of the ice road leading to Seal Island. Mid-way into the experiment, it was necessary

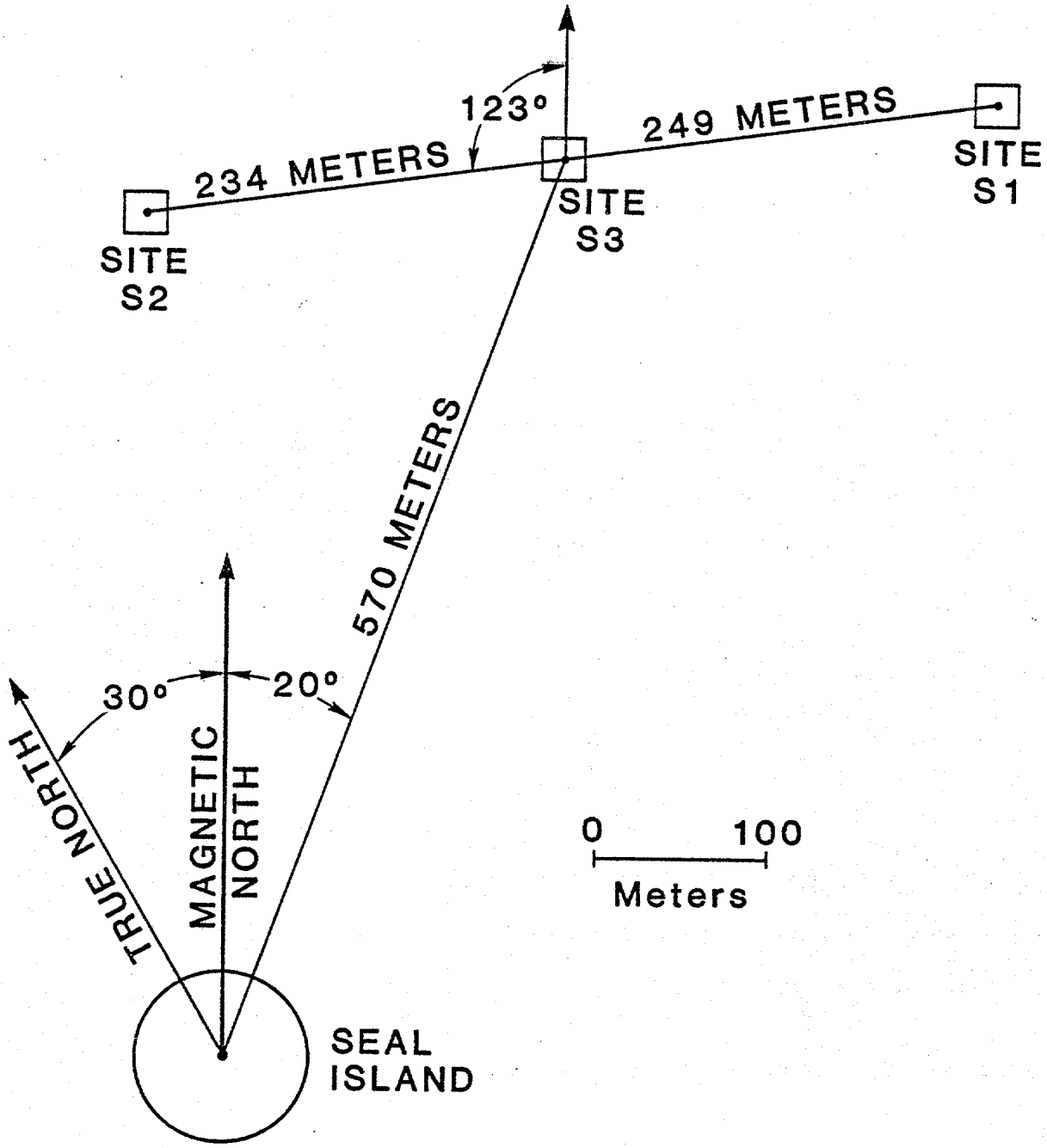

Figure 1. Station Deployment Map.

from the logistics standpoint for Shell Oil Company to move the instrument building from the island surface location to a new location on the ice sheet adjacent to the island. When the ice road began to deteriorate, Shell personnel had to move the instrument building back to the shoreline, and thus the experiment was terminated. The heat generated in each strain gauge bridge was beginning to cause some brine accumulation around each of the uniaxial gauges at this time, implying that decoupling of the ice stress gauge from the ice sheet at the -6°C temperature was imminent.

As described in the Fifth Quarterly Report, some 16 tapes of digital data were collected during the 50 day interval and were subsequently analyzed.

During the interval May through July 1983, additional laboratory calibrations were conducted by Dr. J. B. Johnson for the uniaxial gauges. In particular, the stress concentration factor was determined as a function of angle of orientation between the axis of the gauge and the applied stress. The results of his calibration experiments are described in great detail in Appendix A of this report, a manuscript of which has been submitted for publication to the Journal of Energy Resources Technology.

II. DATA ANALYSIS

Examination of the 16 digital tapes of data collected during the experimental period revealed that the ice stress changes did not exceed 0.7 psi during any of the time interval when data was being recorded. This observed change represented five incremental units of ice stress, as the resolution limit of the ice stress instrumentation system was 0.15 psi. The typical sort of trace obtained from analysis of the ice

stress record is shown in Figure 2. From the analysis of this data, it must be concluded that there were no intervals of high ambient ice stress produced by nature during the period of active data collection. In spite of this, there were some intervals when the more sensitive strain gauges were showing peculiar strain deformations in the ice on several channels simultaneously, but it has not been possible to determine the causes of these very low levels of strain. Figure 3 illustrates the data recorded on some of the strain channels at such low levels. Inasmuch as detailed interpretation of the low level strains in the ice would very likely not contribute to the ultimate objective of the contract, which was to determine ice stress levels in the vicinity of offshore islands, further analysis of the strain data was deferred.

III. RESULTS AND CONCLUSIONS

During the course of the research described above, an ice stress and strain measurement system was successfully designed, built, and deployed in the vicinity of the Shell Oil Company's Seal Island northwest of Prudhoe Bay. Mathematical techniques were developed for the interpretation of ice stress data from a rosette of uniaxial ice stress gauges. Additional mathematical interpretation of data from a array of 9 strain sensors embedded in ice was also completed. The integral method for the interpretation of total force upon offshore islands and structures, in relation to stresses observed in the ice sheet surrounding the structure, was developed. The calibration of uniaxial gauges as a function of angle between the gauge axis and the applied stress was completed. It was also discovered that the presence of an artificial offshore island consistently modifies the boundary of

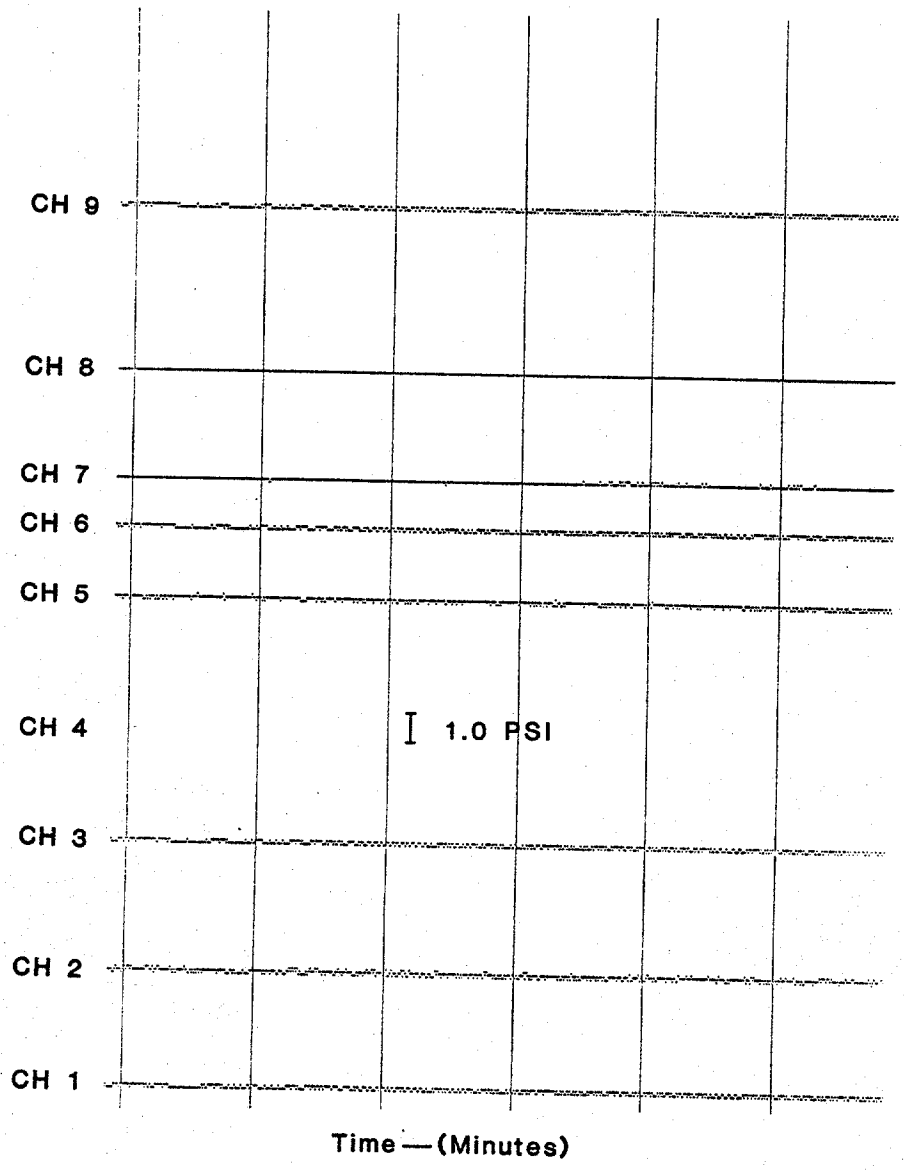

Figure 2. Typical Ice Stress Trace

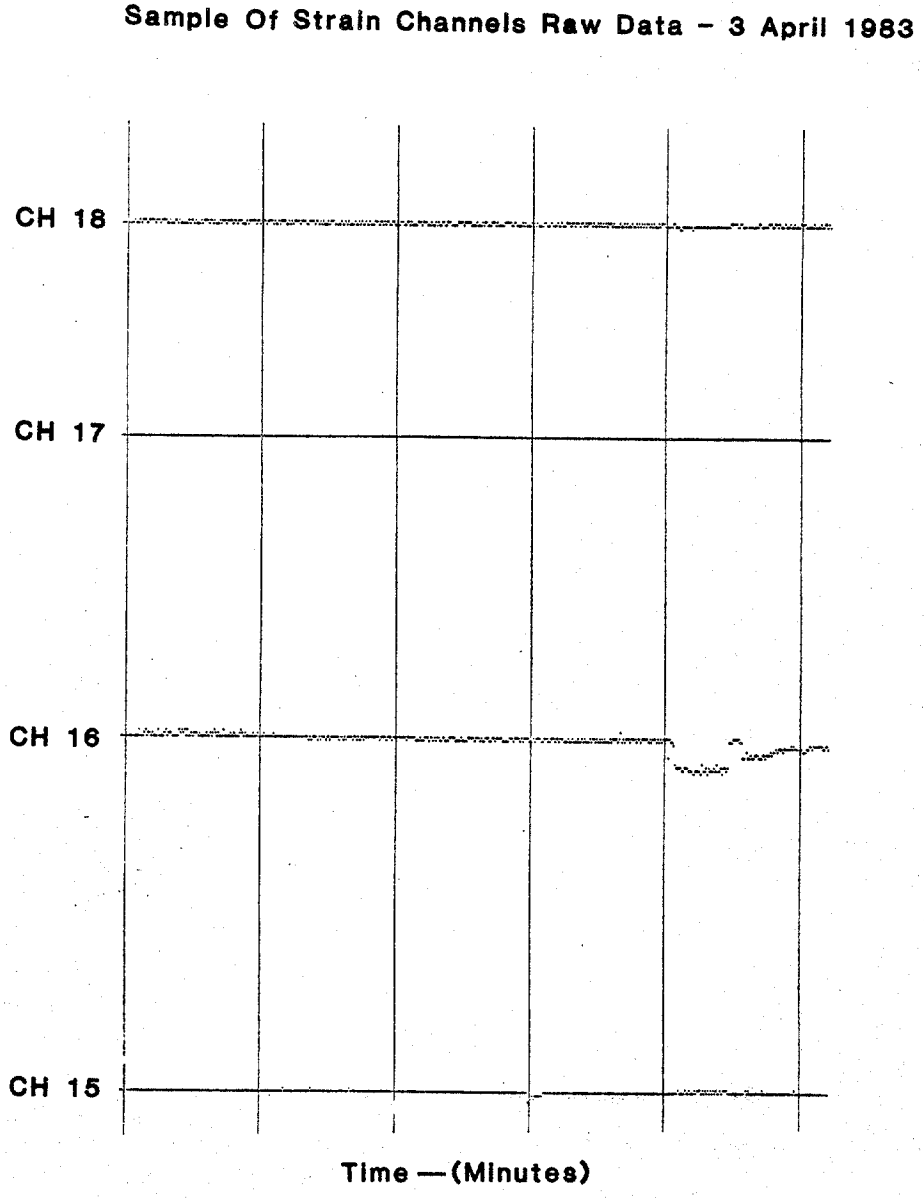

Figure 3(a). Examples of Low Level Strain Data.

the shorefast ice zone, extending it to a location further offshore very early in the winter season. This has the effect of reducing the amount of ice movement for parts of the winter season when the ice is thicker, and can be expected to result in a beneficial reduction of ice force against artificial islands and structures at least out to water depths of the order of 20 m where grounding normally takes place each year. An alternative viewpoint of this phenomenon is that fracturing and ridging against the boundaries of artificial islands and structures takes place during the early part of the winter, when the ice thickness is 10 cm - 30 cm, after which the island serves to define or extend the seaward boundary of the shorefast ice, thus inhibiting additional movement and also preventing the intrusion of multi-year flows from the pack ice during mid-winter. Unfortunately, no large ice stress events took place during the data collection period, and therefore it was not possible to estimate the amount of ice stress in the vicinity of the artificial island which one might encounter during an ice ridging event near the island. Ice stresses during the active data gathering period were below 0.7 psi.

IV. RECOMMENDATIONS

Inasmuch as the ridging of ice takes place routinely around the boundaries of artificial and natural islands early in the winter season, when the ice thickness is in the range 10-30 cm, it is clear that any measurements of ice forces against islands and structures should be done during the period when the ice is highly mobile. A cooperative program has evolved with the Technical Research Centre of Finland to simultaneously measure ice stress in the ice sheet adjacent to the KEMI

I lighthouse in the Gulf of Bothnia, and to measure lighthouse deflection. From earlier calibration experiments, the force/deflection relationship for the lighthouse is known, and the transfer function from an ice sheet to a cylindrical structure can be determined.

With the obvious successful resistance of artificial islands to lateral ice forces since 1972, involving over 30 islands, it is clear that the forces due to annual ice are highly variable but are below the limits related to island failure.

Of more significance for the future is the force on islands and structures in water depths greater than 20 meters. Panels on such structures should be used, and novel rapidly deployed ice instrumentation (e.g. accelerometers) on the ice surface may be related to the forces registered by the panels. A modified experimental approach is required. The forces during interactions between structures and large multi-year floes and ice islands seem to be the major remaining Arctic design questions. Further research could use this approach in full scale, or could use the KEMI I lighthouse with its new conical waterline shell structure as a 1/5-scale model for the deep water Arctic prototype. Valuable design data can thus be obtained from further research involving cooperation with Finland. Full-scale research projects in cooperation with American industry are also very worthwhile. Both avenues of research are recommended.

References

1. Sackinger, W.M. 1982. "Ice Forces Against Arctic Offshore Structures". First Quarterly Report to US Army Cold Regions Research and Engineering Laboratory, and to US Department of Interior, Minerals Management Service, March 1982.

2. Sackinger, W.M. and J.B. Johnson. 1982. "Ice Forces Against Arctic Offshore Structures". Second Quarterly Report to US Army Cold Regions Research and Engineering Laboratory, and to US Department of Interior, Minerals Management Service, June 1982.

3. Johnson, J.B. "A Surface Integral Method for Calculating Ice Loads On Offshore Structures from In-Situ Measurements". Annals of Glaciology, 4, pp. 124-128.

4. Sackinger, W.M. and J.B. Johnson. 1982. "Ice Forces Against Arctic Offshore Structures". Third Quarterly Report to US Army Cold Regions Research and Engineering Laboratory, and to US Department of Interior, Minerals Management Service, September 1982.

5. Sackinger, W.M. and J.B. Johnson. 1983. "Ice Forces Against Arctic Offshore Structures". Fourth Quarterly Report to US Army Cold Regions Research and Engineering Laboratory, and to US Department of Interior, Minerals Management Service, March 1983.

6. Sackinger, W.M. and J.B. Johnson. 1983. "Ice Forces Against Arctic Offshore Structures". Fifth Quarterly Report to US Army Cold Regions Research and Engineering Laboratory, and to US Department of Interior, Minerals Management Service, June 1983.

APPENDIX A

In-ice Calibration Tests for an Elongated, Uniaxial Brass Ice Stress Sensor

J.B. Johnson
US Army Cold Regions Research and
Engineering Laboratory

(In, Proc. of the Fourth International Offshore Mechanics and Arctic Engineering Symposium, February 17-21, 1985, Dallas, TX.)

IN-ICE CALIBRATION TESTS FOR AN ELONGATED, UNIAXIAL BRASS ICE STRESS SENSOR

Jerome B. Johnson
U.S. Army Cold Regions Research and
Engineering Laboratory
Hanover, NH

ABSTRACT

An elongated, uniaxial brass ice stress sensor has been developed by the University of Alaska and used in several field experiments. Laboratory calibration tests have been conducted, in a 60 x 29.5 x 8.5 in. (1524 x 750 x 216 mm) ice block into which the sensor was frozen, to determine the sensor's response characteristics. Test results indicate that the sensor acts as a stress concentrator with a stress concentration factor of 2.4 and transverse sensitivity of -1.3 at stresses below 30 lbf/in.^{2} (207 kPa). At stresses greater than 30 lbf/in.^{2} (207 kPa) the stress concentration factor increased and the sensor exhibited a time delay response to load. Differences of 22% were measured between the measured sensor stress immediately after a constant ice load was applied and the asymptotic stress limit. Interpretation of measured sensor stresses can be considered reliable at ambient ice stress levels below 30 lbf/in.^{2} (207 kPa).

INTRODUCTION

Ice stress is recognized as an important factor in the design of marine and hydraulic structures, ice drift, ride-up, pile-up, pressure ridge formation and pressures in reservoirs. Cox and Johnson [1] reviewed the design and response characteristics of several sensors that have been built to measure stresses in an ice sheet.

One of the early stress sensor designs was developed at the University of Alaska. Nelson [2] and Nelson et al. [3] described the design requirements and experimental test results for an elongated, uniaxial brass ice stress sensor. The sensor was constructed from a brass bar with a reduced diameter section. Strain gauges are attached to the reduced diameter section such that all arms of the strain bridge are active. A copper sheathing covering and a waterproofing compound protect the electronics. End-caps extend from the ends of the transducer to provide tension gripping in the ice (Fig. 1). The initial development and calibration of the sensor was conducted using a 3 in. (76 mm) long by 1 in. (25.4 mm) diameter gauge with a 1 in. (25.4 mm) reduced diameter section 2-1/2 in. (63.5 mm) in length [3].

Direct load calibration tests were conducted by Nelson et al. [3] and included creep loading, rapid loading, and loading until the ice block failed. These tests indicated that the stress concentration factors varied from 3.4 to 6.4 depending on the type of test conducted. The stress concentration factor, α, is defined as the ratio of the measured stress to the applied stress when the long axis of the sensor is oriented in the loading direction. These tests also demonstrated that the sensor was sensitive to loads applied perpendicular to the long axis. This transverse sensitivity varied between -1.53 and -0.082, depending on loading conditions. The transverse sensitivity, β, is defined as the ratio of the measured stress to the applied stress when the long axis of the sensor is oriented normal to the loading direction.

The uniaxial stress sensor has been used in several field experiments to estimate ice stresses near grounded objects, thermal and tide-generated stresses in shorefast sea ice, and stresses associated with ice movement and deformation [4,5,6]. These studies utilized 5 in. (127 mm) long by 2 in. (50.8 mm) diameter sensors as shown in Figure 1. Stress sensor measurements were interpreted by assuming a constant stress concentration factor, α, equal to 3.2 and ignoring the transverse sensitivity ($\beta = 0$). The uniaxial sensor has also been used to measure ice

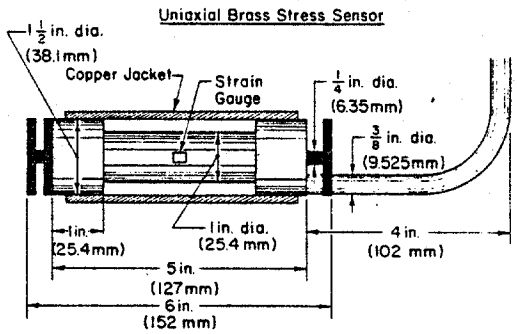

FIG. 1. Elongated, uniaxial brass ice stress sensor.

stresses around offshore structures off the north coast of Canada and Alaska in 1983 and near the coast of Finland in 1984 (Sackinger, personal communication). Past and current interest in utilizing the uniaxial brass stress sensor to measure ice stress points out the need to define the sensor's response characteristics, which have not been well defined or fully utilized. Calibration test results by Nelson et al. [3] showed that α and β varied significantly, even when loading test conditions were similar. In addition, analytical analyses of an elongated inclusion inserted into an elastic plate indicate that the stress concentration factor for the uniaxial stress sensor may depend on θ, the angle between the principal stress axis and the long axis of the gauge [7]. Past field experiments using the uniaxial sensor have used data reduction techniques that have ignored the transverse sensitivity of the gauge. These stress measurements may be suspect unless the contribution of transverse sensitivity is negligible.

The present paper presents the results of a calibration test program that was designed to resolve some of the questions raised above about the uniaxial sensor's response to applied loads. The procedure was to: 1) determine experimentally the sensitivity of the uniaxial sensor (change in sensor electrical output per unit change in applied load) before it was embedded in an ice block; 2) determine experimentally the in-ice stress concentration factor of the sensor as a function of θ; 3) determine experimentally the in-ice transverse sensitivity of the sensor; and 4) present an analytical technique for interpreting the in-ice stress sensor calibration results.

TEST PRODCEDURES

Calibration tests were conducted using a uniaxial sensor with dimensions identical to the sensors that were used in earlier field experiments (Fig. 1). The two basic tests that were conducted included a direct load test on the sensor and loading an ice block into which a sensor had been frozen. The direct load test was conducted by placing weights on one of the endplates of the sensor while the other endplate was held in a vise. The load was cycled several times in an effort to determine the stress sensor's sensitivity, linearity, and hysteresis characteristics. The second test was conducted by freezing the uniaxial sensor into a large freshwater ice block, which was then uniaxially loaded by a hydraulic ram. The ice block was 60 in. long, 29.5 in. wide, and 8 in. thick (1524 x 750 x 216 mm) (Fig. 2). These dimensions were chosen so that the stress disturbance in the ice block due to the presence of the sensor was not felt at the boundaries of the block. The use of an ice block of sufficiently large dimensions is necessary to ensure that the block can adequately represent an infinite ice sheet and thereby reduce the variability of the test results. Nelson et al. [3] used an 8 x 8 x 12 in. (203 x 203 x 304 mm) block for their tests on a 3 x 1 in. (76 x 25 mm) diameter gauge. This small block size may account for some of the variability of their results.

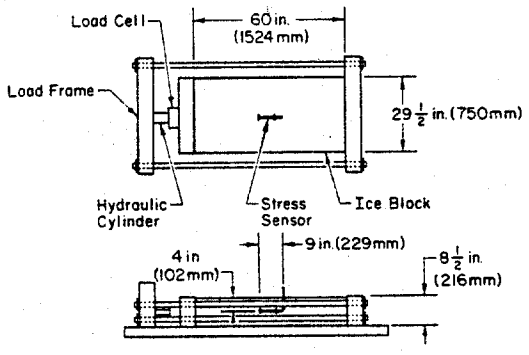

FIG. 2. Experimental test setup for the load frame, ice block, and stress sensor.

Freshwater ice was used for convenience; however, the results should be applicable to saline ice as well. The uniaxial stress sensor was designed to be stiff as compared to ice (i.e. to have an elastic modulus much greater than that of freshwater or saline ice). Nelson [2] has shown analytically that the stress concentration factor of a stiff elongated stress sensor is little affected by changes in the modulus or by creep of the ice. These results are supported by experiments on stiff cylindrical stress sensors which were embedded in both freshwater and saline ice [1,8]. The experiments indicate that differences in the elastic modulus and creep behavior for freshwater and saline ice do not significantly affect the behavior of a stiff stress sensor.

The freshwater ice block used in this experiment was grown in the loading frame (Fig. 2). The base of the frame consisted of a 1 in. (25.4 mm) thick sheet of plywood that was covered with a double layer of plastic sheeting. The plastic sheeting provided a watertight membrane during freezing and a low friction surface under the ice block during loading. The sidewalls of the ice growing frame were also made from plywood. The plywood was coated with a lubricating grease to prevent the ice from bonding during ice growth. The loading platens at the ends of the load frame were covered with a double layer of plastic sheeting. The uniaxial sensor was placed at mid-depth in the center of the framework and allowed to freeze in place. Once the ice block was made, the plywood sidewall supports were removed. The ice block was then loaded using a 100,000 lbf (45 MN) hydraulic cylinder. The loads were monitored with a 150,000 lbf (67 MN) load cell that was mounted in series with the hydraulic cylinder. The load cell was calibrated by the manufacturer and was found to respond linearly over the full range of loads used in the calibration test. Loads were accurately resolved to 150 lbf (670 N) which corresponds to a stress of 0.6 lbf/in.^{2} (4 kPa). Initially it was planned to run all loading experiments to a maximum stress of 100 lbf/in.^{2} (689 kPa). As preliminary tests resulted in a shear failure between the loading platens, the maximum stress was limited to 30 lbf/in.^{2} (207 kPa) for the majority of tests. The applied stress was increased to 70 lbf/in.^{2} (483 kPa) for the final test series with the sensor's long axis aligned parallel to the direction of the applied stress, $\theta = 0°$.

Tests were conducted at an ice block temperature of 23°F (-5°C) with the sensor at five different orientations to the applied stress. The sensor was first tested at $\theta = 0°$. A chain saw was used to remove the sensor from the ice. The sensor was then reoriented to $\theta = 30°$ and refrozen into the center of the block, and another set of tests were conducted. This procedure was repeated for $\theta = 45°$, 60°, and 90°. There was some concern that removing the sensor from the ice block and then refreezing it into the block might alter the test conditions. The effect of the removal/installation process was examined by conducting the final test series by removing the gauge after

the $\theta = 90°$ test and refreezing it at $\theta = 0°$. The results of the last test series were then compared with those of the first test with $\theta = 0°$ and found to be the same within the limits of experimental error.

Both rapid-loading and creep tests were conducted on the ice block into which the sensor was embedded. The rapid-loading tests were performed by increasing and then decreasing the load incrementally. The load was allowed to stabilize briefly before being changed. Creep tests were conducted by increasing the applied load to a given level and maintaining it until the stress sensor response was stable.

The excitation voltage for the strain gauge bridge mounted on the sensor was set at 6 V. This is the same level that has been used in all past field experiments. The load information from the load cell and stress sensor were recorded on an x-y plotter. The data presented here are based on the x-y plotter records.

DATA REDUCTION AND TEST RESULTS

Stress sensor load sensitivity was determined from the direct loading test. These results indicate that the sensor response is repeatable, linear and had little hysteresis (Fig. 3). The load sensitivity for these tests was given by

$$\Delta F = G\ S\ E_0 = (1.27\ \text{lb}/\mu\text{V})\ E_0$$

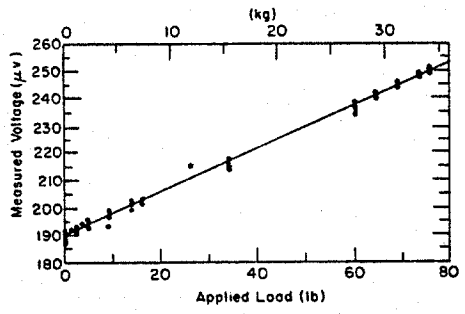

FIG. 3. Load sensitivity for the uniaxial brass ice stress sensor from direct loading tests.

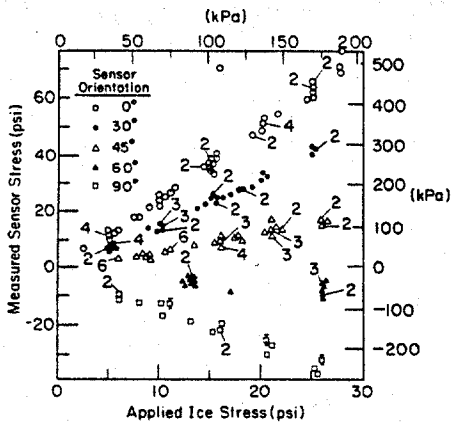

FIG. 4. Results of low-magnitude stress-loading tests in ice. The number of separate measurements taken at a given applied stress are shown in the figure.

Table 1. Summary of Statistics on Calibration Data.

Least Squares Fit to Data

Stress sensor orientation to loading (deg)	Correlation coefficient	Slope	Vertical axis intercept	Standard deviation about the slope*
0	0.95	2.4	2.1	0.1
30	0.99	1.7	-1.8	0.2
45	0.99	0.7	-0.9	0.1
60	-0.58	-0.2	-2.0	0.1
90	-0.98	-1.3	-1.6	0.2

* The slope is also the mean ratio of measured sensor stress and applied ice stress.

where ΔF is the change in load, G is the amplification gain, S is the load sensitivity coefficient, and E_0 is the sensor output in volts. Measured stresses were determined by dividing the load sensitivity of the sensor by the surface area of the endcaps:

$$\sigma_m = \Delta F/A\ .$$

Applied ice block stresses were determined by dividing the measured load from the load cell by the cross sectional area of the ice block. The test results are presented in four different formats to illustrate the behavior characteristics of the sensor. The original test results for stress sensor orientations of 0°, 30°, 45°, 60°, and 90° to the principal stress direction are shown in Figure 4. A linear least squares method was used to fit a line to each of the data sets shown in Figure 4. The coefficients determined from the least squares fit are presented in Table 1. The slope of the fitted line is also the mean value of the ratio of measured sensor stress to applied ice block stress. The slope of the fitted curve for $\theta = 0°$ is the mean stress concentration factor; it was found to be 2.4 with a standard deviation of 0.1. The mean transverse sensitivity of the sensor was determined from the slope of the fitted curve at $\theta = 90°$ and was -1.3 with a standard deviation of 0.2.

The results shown in Figure 4 indicate that the sensor response was generally linear in each orientation. However, the magnitude of the applied stress that was detected by the sensor did depend on orientation. This behavior was expected since the sensor was designed to sense stresses along its axis, and these would vary depending on the orientation of the sensor to the applied load. Nelson et al. [3] suggested that the measured sensor stress could be related to the applied stress by a Mohr's circle representation. For a uniaxial stress field, the ratio of measured stress, σ_m, to applied stress, σ_a, can be given by

$$\sigma_m/\sigma_a = (\alpha \cos^2\theta + \beta \sin^2\theta)\ . \qquad (1)$$

Figure 5 is a plot of the mean value of σ_m/σ_a for each test orientation. The standard deviation about the mean is delineated by the bars extending from the data points. The calculated curve for σ_m/σ_a is also plotted:

$$\sigma_m/\sigma_a = 2.4 \cos^2\theta - 1.3 \sin^2\theta$$

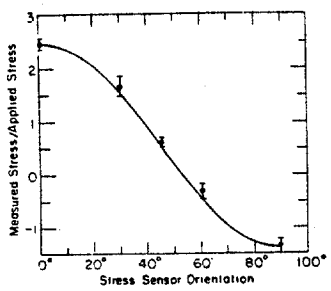

FIG. 5. Measured sensor stress to applied ice-stress ratio as a function of stress sensor orientation to the principal stress direction.

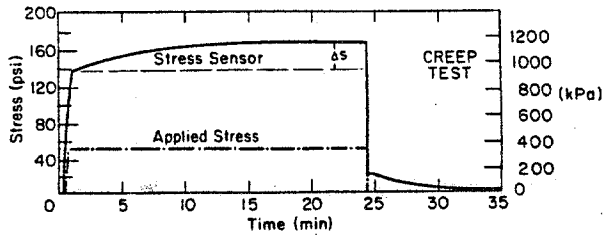

FIG. 6. Creep loading test results. The difference between the initial measured stress after imposing a constant applied stress and the asymptotic limit of the measured stress is shown by ΔS.

where the stress concentration factor at 0° is 2.4 and the tangential sensitivity of the sensor at 90° is -1.3. The calculated results agree with equation 1, supporting Nelson's suggestion that the measured stress/applied stress ratio can be represented by the Mohr circle theory.

The typical response of the uniaxial ice stress sensor to a constant load as a function of time is shown in Figure 6. Here the measured sensor stress increases as the applied ice stress is increased to a constant 50 lbf/in.^{2} (346 kPa) magnitude. The measured stress then continues to increase asymptotically to a limiting value as the time increases. The difference between the measured sensor stress immediately after the applied stress reached a constant value and the asymptotic limit of the measured sensor stress was 22% (ΔS in Fig. 6). The sensor did not exhibit a time-dependent response to load during the direct loading test. This indicates that the time response of the sensor in ice must be due to the interaction of ice and sensor. The sensor configuration may produce its time-dependent response in ice to creep loading. The endcaps of the sensor are designed so that ice will form around them, allowing the sensor to respond to both compressive and tensile stresses. The ice that fills the region between the backside of the endplates and the body of the sensor may support some of the applied ice stress through shear to the main ice sheet. As the applied load is maintained, the ice plug may begin to creep, allowing the sensor to gradually assume the full load due to the applied ice stress. Test results indicate that the sensor's time-dependent response to creep loading is more severe at higher applied stresses.

A final test was performed at θ = 0° to examine the relationship between the stress concentration factor and the magnitude of the applied stress. This was the only test sequence that was conducted at stress levels greater than 30 lbf/in.^{2} (207 kPa). At these higher stress levels, noticeable cracking of the ice near the loading platens was observed. Eventually, cracks formed in the body of the block, and the test was ended. The test results indicated that the stress concentration factors were scattered in a range that was consistent with α = 2.4 when the applied ice stress was 30 lbf/in.^{2} (207 kPa) or less. At stress levels between 30 lbf/in.^{2} (207 kPa) and 70 lbf/in.^{2} (483 kPa) the stress concentration factors increased to more than 3 (Fig. 7). The larger stress concentration factors at higher loads may be due to local ice cracking around the sensor, which resulted in increased load transfer to the sensor. Too few tests were conducted to fully document the relationship between the stress concentration factor and applied stress. However, the available results are generally consistent with the findings of Nelson et al. [3] and indicate that different α values should be used to interpret measured stresses correctly, depending on the loading conditions and stress magnitude (for example, rapid loading, creep loading, or loading to ice block failure).

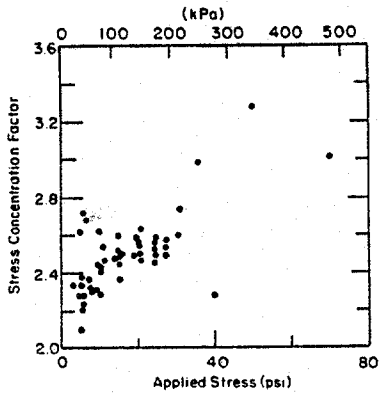

FIG. 7. Stress concentration factor as a function of the applied ice stress for θ = 0° configuration.

IMPLICATION OF CALIBRATION TEST RESULTS ON DATA INTERPRETATION

The calibration test results described in the previous section indicate that at applied ice stresses below 30 lbf/in.^{2} (207 kPa), the measured stresses can be reasonably described by using a Mohr's circle representation of the sensor response and constant values for α and β. At stress levels above 30 lbf/in.^{2} (207 kPa) the time-dependent response characteristics and the dependence of α on the applied ice stress of the uniaxial stress sensor become important.

For relatively low ambient ice-stress levels, the Mohr circle representation suggested by Nelson et al. [3] can be used to interpret field data. The measured ice stresses can be related to the principal stresses in a biaxial stress field by

$$\sigma_m = (\alpha+\beta)\frac{p_1+p_2}{2} + (\alpha-\beta)\frac{p_1-p_2}{2}\cos 2\theta$$

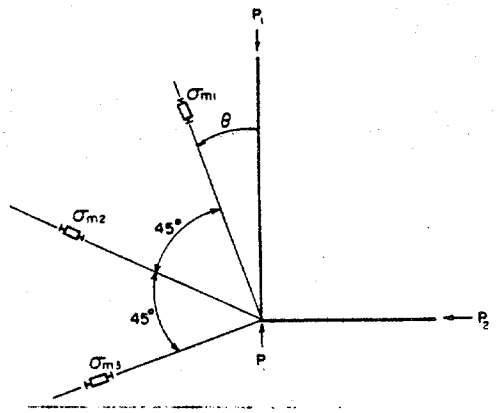

FIG. 8. Stress sensor rosette used to determine the magnitude and direction of the principal stresses.

where p_1 and p_2 are the primary and secondary principal stresses acting on an ice sheet. The principal stresses p_1 and p_2 acting on an ice sheet can be determined by using a rosette of three stress sensors embedded in the ice. If the sensors have an angular separation of 45° as shown in Figure 8, then

$$p_1 = \frac{\sigma_{m_1} + \sigma_{m_3}}{2(\alpha+\beta)} + \frac{[(\sigma_{m_1} - 2\sigma_{m_2} + \sigma_{m_3})^2 + (\sigma_{m_1} - \sigma_{m_3})^2]^{1/2}}{2(\alpha-\beta)}$$

$$p_2 = \frac{\sigma_{m_1} + \sigma_{m_3}}{2(\alpha+\beta)} - \frac{[(\sigma_{m_1} - 2\sigma_{m_2} + \sigma_{m_3})^2 + (\sigma_{m_1} - \sigma_{m_3})^2]^{1/2}}{2(\alpha-\beta)}$$

$$\tan 2\theta = \frac{\sigma_{m_1} - 2\sigma_{m_2} + \sigma_{m_3}}{\sigma_{m_1} - \sigma_{m_3}}$$

In previous field experiments ice stresses have been calculated without considering the effects of the sensor's transverse sensitivity. The calculated angle of orientation, θ, will not be affected since β does not enter into the formula. The calculated p_1 and p_2 values may, however, be in error. The errors for p_1 and p_2 in a biaxial stress field can be derived from the above equations and are given by

$$\Delta p_1 = -\frac{\beta}{\alpha} p_2 \quad \text{and} \quad \Delta p_2 = -\frac{\beta}{\alpha} p_1$$

where $\Delta p_1 = (p_1)_{\alpha,\beta} - (p_1)_{\alpha,0}$ and $\Delta p_2 = (p_2)_{\alpha,\beta} - (p_2)_{\alpha,0}$. Δp_1 and Δp_2 are the differences between the calculated principal stresses, assuming the influence of both α and β, and the calculated principal stresses, assuming no transverse sensitivity. For $\alpha = 2.4$ and $\beta = -1.3$, as were determined from the calibration tests, we have

$$\Delta p_1 = 0.52\, p_2 \quad \text{and} \quad \Delta p_2 = 0.52\, p_1.$$

The percentage error is determined by dividing by the principal stresses where

$$\frac{\Delta p_1}{p_1} = 0.52\, \frac{p_2}{p_1} \quad \text{and} \quad \frac{\Delta p_2}{p_2} = 0.52\, \frac{p_1}{p_2}.$$

These results show that the errors associated with setting $\beta = 0$ depend on the biaxial stress ratios p_2/p_1 and p_1/p_2 and can be significant. The calculated stresses can differ up to 52% from actual ice stresses by assuming $\beta = 0$. This indicates that the transverse sensitivity factor should be taken into account in all calculations where the direction and magnitudes of the principal stresses are not known. The errors associated with assuming $\beta = 0$ can be reduced or eliminated in special situations when the secondary principal stress, p_2, is known to be negligible.

Interpretation of measured sensor stress becomes difficult at higher stress magnitudes because of a variation of stress concentration factor with applied stress. Additional calibration tests need to be conducted to better define the applied ice-stress/stress concentration factor relationship and determine if it is repeatable. If the increase in the stress concentration factor is due to local fracturing around the sensor it is doubtful that any applied ice-stress/stress concentration factor relationship will be repeatable. However, one possible method of interpreting measured stresses would be to calculate ice stress using the low stress level α. The calculated stress magnitude could then be used to estimate the appropriate α value to be used in estimating the final stress magnitudes. This is not a very satisfactory method of determining in-situ stresses, and the calibration test results indicate that measured sensor stresses should be viewed with caution when the applied ice stresses are greater than 30 lbf/in.^{2} (207 kPa).

CONCLUSIONS

The elongated, uniaxial brass ice stress sensor does respond to low-level ice stresses in a predictable manner. The calibration tests conducted in this study indicate that, for ice stresses less than 30 lbf/in.^{2} (207 kPa), the ice stress sensor exhibits a stress concentration factor of 2.4 and transverse sensitivity factor of -1.3. The ratio of the measured stress and applied stress can also be described by a Mohr circle representation. The stress concentration factor was found to increase with increasing ice stress for applied stresses in excess of 30 lbf/in.^{2} (207 kPa). This behavior was attributed to localized ice failure near the sensor. Additional loading tests are required to better define the relationship between stress concentration factor and applied stress. The sensor also exhibited a time-delayed response to constant applied stresses greater than 50 lbf/in.^{2} (347 kPa). Time delays of up to 20 min. were required for measured sensor stresses to asymptotically approach a stable value after the application of a constant ice stress.

Field experiments utilizing the uniaxial sensor need to be carefully designed to ensure that the ice-stress magnitudes do not exceed the levels at which measured sensor stresses can be confidently calculated. The calibration test results indicate this upper limit of ice stress to be 30 lbf/in.^{2} (207 kPa). Past field experiments have used a stress concentration factor of 3.2 and have ignored the transverse sensitivity when calculating ice stresses. The stress concentration factor determined in this study is believed to be more reliable than the 3.2 value since earlier experiments were conducted using smaller stress sensors and the test ice-block dimensions were

too small to incorporate the stress disturbance due to the embedded sensor. The earlier experiments showed greater variability in results than was obtained in this study. Calculated ice-stress magnitudes may have significant errors when the effects of transverse sensitivity are not accounted for. The magnitude of these errors depends on the stress concentration/ transverse sensitivity ratio for the sensor and the ratio of primary to secondary principal stress. The calibration tests indicate that errors of up to 52% may occur for the uniaxial sensor, when the transverse sensitivity of the sensor is not included in the analysis of measured stresses.

ACKNOWLEDGMENT

This work was supported by the Minerals Management Service, U.S. Department of the Interior. I express my appreciation to Dr. William M. Sackinger for his encouragement and support while conducting this study, to Mr. Dan Solie for assisting with the experiments and to Dr. Gordon F.N. Cox and Dr. Devinder S. Sodhi for technically reviewing the report.

REFERENCES

1. Cox, G.F.N. and Johnson, J.B. Stress Measurements in Ice, U.S. Army Cold Regions Research and Engineering Laboratory, CRREL Report 83-23, Hanover, N.H., 1983, 31 pp.

2. Nelson, R.D. Internal Stress Measurements in Ice Sheets Using Embedded Load Cells, in Proceedings of the 3rd International Conference on Port and Ocean Engineering Under Arctic Conditions: University of Alaska, Fairbanks, Vol. 1, 1975, pp. 361-373.

3. Nelson, R.D., Tauriainen, M. and Borghorst, J. Techniques for Measuring Stress in Sea Ice, University of Alaska, Alaska Sea Grant Report No. 77-1, 1977, 65 pp.

4. Nelson, R.D. Measurement of Tide and Temperature-Generated Stresses in Shorefast Sea Ice, in The Coast and Shelf of the Beaufort Sea (J.C. Reed and J.C. Slater, eds.), Arctic Institute of North America, 1974, pp. 195-204.

5. Rogers, J.C., Sackinger, W.M. and Nelson, R.D. Arctic Coastal Sea Ice Dynamics, in Proceedings of the Offshore Technology Conference, May 6-8, Houston, Texas, Vol. 2, paper No. 2047, 1974, p p. 133-144.

6. Sackinger, W.M. and Nelson, R.D. Measurements of Sea-Ice Stresses Near Grounded Obstacles, Journal of Energy Resources Technology, Vol. 102, no. 3, 1980, pp. 144-147.

7. Savin, G.N. Stress Concentrations around Holes: New York, Pergamon Press, 1961, 430 pp.

8. Johnson, J.B. and Cox, G.F.N. The OSI Ice Stress Sensor, In Proceedings of the Workshop on Sea Ice Field Measurements, St. John's, Newfoundland. Center for Cold Oceans Resources Engineering, C-CORE Report 80-21, 1980, pp. 193-207.

APPENDIX B

A Surface Integral Method for Determining Ice Loads on Offshore Structures from In Situ Measurements

J.B. Johnson
Geophysical Institute, University of Alaska
Fairbanks, Alaska

In, Annuals of Glaciology, 4, 1983).

Annals of Glaciology 4 1983

A SURFACE INTEGRAL METHOD FOR DETERMINING ICE LOADS ON OFFSHORE STRUCTURES FROM *IN SITU* MEASUREMENTS

by

Jerome B. Johnson
(Geophysical Institute, University of Alaska, Fairbanks, Alaska 99701, U.S.A.)

ABSTRACT

Two methods are presented for calculating ice loads on structures using measurements from sensors imbedded in a floating ice sheet and from instruments attached to a structure. The first method uses a mathematical model describing ice/structure interaction for a cylindrical structure to interpret stress measurements. This technique requires only a few sensors to develop an estimate of ice loads. However, analytical and experimental results indicate that using a mathematical model to interpret stress measurements can result in inaccurate load estimates due to uncertainty in the accuracy of the model and and the uncertainty of using local ice stresses to calculate total ice forces. The second method of calculating ice loads on structures utilizes Euler and Cauchy's stress principle. In this, the surface integral method, the force acting on a structure is determined by summing the stress vectors acting on a surface which encompasses the structure. Application of this technique requires that the shear and normal components of stress be known along the surface. Sensors must be spaced close enough together so that local stress variations due to the process of ice failure around a structure can be detected. The surface integral method is a useful technique for interpreting load and stress measurements since a knowledge of the mechanism of ice/structure interactions is not needed. The accuracy of the method is determined by the density of sensors along the surface. A disadvantage of the technique is that a relatively large number of sensors are needed to determine the stress tensor along the surface of interest.

The surface integral method can be used to examine the effects of grounded ice rubble on structural ice loads. Two instrumented surfaces, one enclosing a structure and the other enclosing the structure and rubble field can be used to estimate the load acting only on the structure and also on the structure/rubble-field system.

INTRODUCTION

Resource exploration and establishing navigational aids in cold offshore regions require bottom-founded structures which can withstand the lateral forces generated by moving ice. Various methods have been used to estimate ice loads on structures including: mathematical analyses of ice interacting with structures (Croasdale and others 1977, Kerr 1978, Ralston 1978[a], [b], and others), small-scale model experiments (Edwards and Croasdale 1977, Lewis and Croasdale 1978), measurements of ice stress in conjunction with mathematical descriptions of the stress field around structures (Semeniuk 1977, Strilchuk 1977) and direct measurements of circumferential loads and bending moments on instrumented structures Danys and Bercha 1976, Määttänen 1978, 1980). Mathematical analyses and small-scale modeling techniques are now the methods that are most used for estimating ice loads. Mathematical models are developed by making certain assumptions about the mechanism of the interaction between a structure and ice, the rheology of ice and the environment which will be encountered. The usefulness of such models depends on how realistic the assumptions are. Small-scale model tests and prototype tests (Verity 1975, Robbins and others 1976) have been used to derive approximate empirical solutions for ice forces on structures. These solutions have then been compared with mathematical models (Kry 1980[b]). A drawback of both scale model tests and mathematical models is that the lack of load measurements for full-size structures limits the extent to which modeling efforts can be compared and verified. The extreme cost and necessary overdesign of a full-scale test structure has limited the number of direct load measurements available. Direct measurements of ice loads have in the past been conducted on structures of relatively small diameter, lighthouses and pilings (Schwarz 1970, Neill 1971, Danys and Bercha 1976, Määttänen 1978). Recent efforts, however, have been directed at determining loads on full-scale, exploratory structures (Semeniuk 1977, Strilchuk 1977, APOA 1981). Determining the ice loads that act on full-scale structures provides important information to the designer including: (1) data to which scale model experiments and mathematical models can be compared, (2) lower bounds to possible ice forces, (3) an historical database which, in conjunction with other environmental parameters, can be used for developing design criteria in probabilistic terms, and (4) information about the influence of ice rubble piles, which surround a structure, on ice forces.

The requirements for directly determining ice loads on structures from in situ measurements have been discussed only briefly in the literature. Essentially two general methods are used. The first method involves measuring the forces acting on a structure using instruments attached to the structure. These can consist of either circumferential load cell or

bending moment measurements and in this paper are referred to as load measurements (instrumented island). Load cells, sensitive to normal forces, are typically placed around the circumference of a structure and the load across the face of the structure is measured (Schwarz 1970, Määttänen 1978). Measurements of the bending moment of a structure have been used to determine ice loading but are difficult to interpret due to low signal output (Määttänen 1978). Instrumented structures are an attractive method for determining ice forces since a knowledge of the mechanism of ice/structure interactions is not required. However, unreliable load estimates can result from the use of sensors which do not respond to the total traction force. Sensors which respond only to the normal component of load without regard for possible contributions from shear loads have been deployed on instrumented structures in the past (Danys and Bercha 1976, Määttänen 1978) and can result in an underestimate of structural loading.

Recent efforts have been made to measure the total traction force on support members of the Yukon River bridge in Alaska and a bridge over the Ottauquechee River in Vermont (Burdick personal communication, Sodhi personal communication). Sensors are used that respond to both normal and shear loads.

A second method of determining structural ice loads involves embedding sensors that respond to stress in the ice around a structure, referred to in this paper as stress measurements (in ice). The resultant ice forces are determined from stress measurements by using a mathematical model describing ice/structure interaction (Strilchuk 1977, Metge and others 1981, Templeton unpublished). The disadvantages of using stress measurements in conjunction with mathematical models are uncertainties concerning the accuracies of the stress measurements, and of the mathematical description for ice/structure interaction, and concerning the use of local ice stresses to calculate total ice forces. Kry (1978[b], 1980[a]) has suggested that ice can fail in independent zones across wide structures. Such failure may result in local ice stresses which are not representative of the average stress acting on the structure. Measurements of ice stress by Strilchuk (1977) provide an example of the difficulty of using local stress measurements to determine the total structural ice force.

Past difficulties of obtaining accurate measurements of ice load for structures illustrates the importance of understanding which forces need to be measured and how in situ measurements should be interpreted. This paper examines the questions associated with the deployment of stress (in ice) and load (instrumented island) sensors and the use of the resulting data to determine structural ice loads. Two methods for determining structural ice forces from in situ measurements are described. The first method uses a mathematical description of ice/structure interaction and has been used previously. The second method uses a surface integral approach to compute total ice forces from in situ measurements. This method is useful because it does not require a knowledge of ice/structure mechanisms and can be applied to any structural geometry. The surface integral method is then used to demonstrate how stress and load measurements can be used to determine the influence of ice rubble piles, which surround a structure, on ice forces.

CALCULATING ICE LOADS

Stress measurements in conjunction with a mathematical model of ice/structure interaction

In situ measurement of ice stresses around offshore structures is a difficult and time-consuming task. The use of a mathematical model to describe the interaction between ice and structure can reduce the number of stress measurements needed to determine ice loads on a structure, provided that the model is realistic. To date, the mathematical models describing ice/structure interactions that are used with stress sensor measurements have been for cylindrical structures. This geometry lends itself to a relatively simple solution when compared to more complicated shapes. The general assumption regarding ice/structure interaction is that an elastic ice sheet moves past a cylindrical structure and the total force of the ice is resisted by the structure (Fig.1). This situation has been described mathematically by Strilchuk (1977) and Wang (1978) and is given by

$$\sigma_r = N_r P \cos\theta \quad (1)$$

$$\sigma_\theta = N_\theta P \cos\theta \quad (2)$$

$$\tau_{r\theta} = N_{r\theta} P \sin\theta \quad \text{for } -\pi/2 \leq \theta \leq \pi/2 \quad (3)$$

and

$$\sigma_r = \sigma_\theta = \tau_{r\theta} = 0 \text{ for } -\pi/2 < \theta < 3\pi/2 .$$

The radial, tangential and shear stresses acting in the ice in polar coordinates are respectively σ_r, σ_θ and $\tau_{r\theta}$. The average pressure acting on the structure along the diameter d-d' is P (Fig.1). The three coefficients N_r, N_θ and $N_{r\theta}$ depend on the boundary condition at the ice/structure interface and are given by

$$N_r = 4/(\pi X) \quad \text{(Strilchuk 1977)}, \quad (4)$$

and for a fixed boundary condition along the ice-structure interface

$$N_r = 1/\pi\ ((1+\nu)/X^3 - (3+\nu)/X), \quad (5)$$

$$N_\theta = 1/\pi\ (-(1+\nu)/X^3 + (1-\nu)/X), \quad (6)$$

$$N_{r\theta} = 1/\pi\ ((1+\nu)/X^3 + (1-\nu)/X), \quad (7)$$

and for a frictionless boundary condition

$$N_r = -1/\pi((1-\nu)/X^3 + (3+\nu)/X), \quad (8)$$

$$N_\theta = 1/\pi((1-\nu)/X^3 + (1-\nu)/X), \quad (9)$$

$$N_{r\theta} = 1/\pi\ (-(1-\nu)/X^3 + (1-\nu)/X), \quad (10)$$

where $X = r/R$ and ν is Poisson's ratio (Wang 1978). The radial distance from the center of the structure to a point in the ice sheet is given by r and the structure radius by R.

In application of the model the radius R is taken as the ice failure boundary. This could be the structure radius or the radius of a frozen annulus of ice around the structure. Measurements of ice movement have been used to determine the direction of movement of the ice sheet and estimate the principal stress direction (Strilchuk 1977). The average load on the structure can be estimated from a stress sensor, which measures stress in the radial direction, located in the region $-\pi/2 \leq \theta \leq \pi/2$ (Fig.1). For example, the average stress acting on the island can be computed from

$$P = \sigma_r'/(N_r \cos\alpha), \quad (11)$$

where σ_r' is the stress reading at SS_1 in Figure 1 and α, the angle between the stress sensor and principal force direction, is determined from measurements of ice movement (Strilchuk 1977).

A second method of estimating P without using measurements of ice movement makes use of an array of four stress sensors, SS_1 to SS_4, with angular spacings of $\pi/2$ around a structure (Figure 1). Using Equation (1) it is easy to show that

$$\alpha = \tan^{-1}(\sigma_r''/\sigma_r') \quad (12)$$

and

$$P = \sigma_r'/(N_r \cos \alpha) \qquad (13)$$

where

$$\sigma_r'' < \sigma_r', \quad \sigma_r''' = \sigma_r'''' = 0$$

and α is the angle between the principal force direction and σ_r'. The stress readings at SS_1, SS_2, SS_3 and SS_4 in Figure 1 are respectively σ_r', σ_r'', σ_r''' and σ_r''''. A four-sensor technique has been discussed by Templeton (unpublished) although the mathematical formulation was not given.

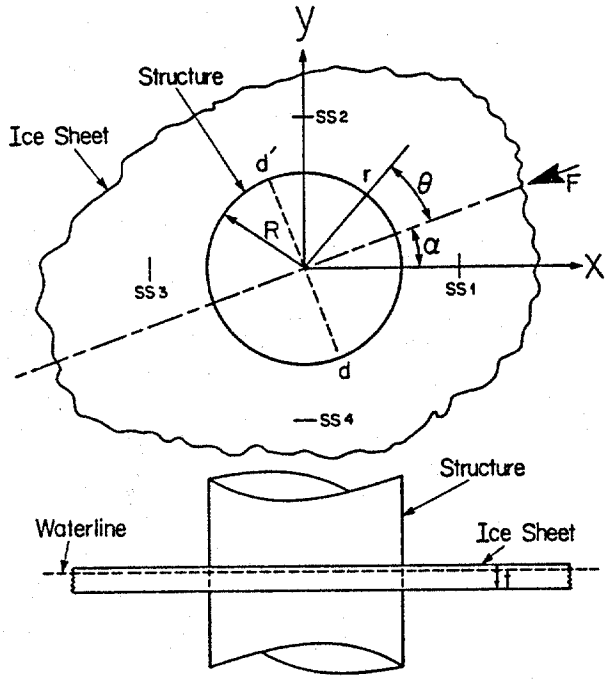

Fig.1. Ice sheet moving past a cylindrical structure.

It is unlikely that the model for ice/structure interaction described by Equations (1), (2) and (3) is adequate to determine structural ice loads from stress sensor measurements. The mechanical properties of ice and the failure mechanisms for ice around wide structures are complex and, in general, not well understood. Measurements of ice stress around three exploration islands in the Canadian Beaufort Sea illustrate the difficulties of using a mathematical model to interpret stress measurements. Several different sensors around the islands were used to calculate independently the average pressure P acting on the islands. P was found to vary significantly depending on the sensor and its location. In some cases the variations in P were greater than 690 kPa for different sensors (Semeniuk 1977, Strilchuk 1977).

The use of mathematical models to interpret stress measurements is probably even less reliable for structures with noncircular geometries (for example, rectangular or polygonal shapes). The stress distribution around such structures can be complex and dependent on the direction of loading. Therefore, it is important to develop methods for interpreting stress and load measurements which do not require an understanding of the details of ice/structure interaction.

The surface integral method for calculating structural loads from in situ measurements

A method for interpreting in situ stress and load measurements that does not require an understanding of of ice/structure interaction can be developed from first principles of continuum mechanics. In the analysis of structural loading only the surface forces or stresses due to the ice acting against a structure are important (body forces can be neglected). The surface force acting on an imagined surface in the interior of a body is the stress vector of Euler and Cauchy's stress principle. According to this concept, the total force acting upon the region interior to a closed surface s is

$$\vec{F} = \oint_S \overset{\upsilon}{T}\, ds, \qquad (14)$$

where $\overset{\upsilon}{T}$ is the stress vector acting on the surface element ds whose outer normal vector is $\vec{\upsilon}$ (Fig.2). The geometry of a structure and the surface of integration s can be any shape. However, for the purposes

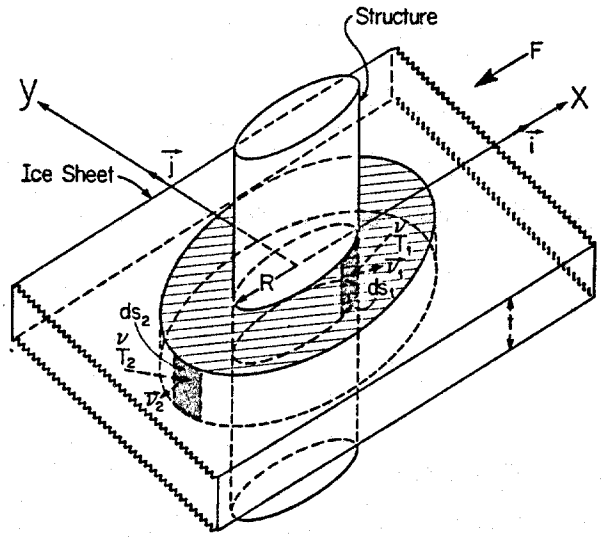

Fig.2. Ice sheet moving past a cylindrical structure. Two surfaces of integration are shown: one along the ice/structure interface and one in the ice sheet surrounding the structure.

of illustration a cylindrical structure and cylindrical surfaces are used in this paper. Figure 2 illustrates the concept of applying the surface integral method for calculating the load on a cylindrical structure. Provided that it encompasses the structure, s can be placed anywhere in the ice sheet. Two possible surfaces of integration shown in Figure 2 include one surface that follows the circumference of the structure S_1 and another in the ice sheet S_2. Once the traction vector (stress vector) is known, the load acting on the body interior to s can be determined. The surface traction vector is defined as

$$\overset{\upsilon}{T} = \vec{\upsilon} \cdot \{\Sigma\} \, . \qquad (15)$$

where the stress tensor of the ice sheet is $\{\Sigma\}$. The stress tensor can be developed in several ways depending on the coordinate system. For the cylindrical structure depicted in Figure 2 in Cartesian coordinates,

$$\{\Sigma\} = [\sigma_{ij}] = \begin{pmatrix} \sigma_x & \tau_{xy} & \tau_{xz} \\ \tau_{yx} & \sigma_y & \tau_{yz} \\ \tau_{zx} & \tau_{zy} & \sigma_z \end{pmatrix} \qquad (16)$$

and

$$\vec{\upsilon} = \cos\theta\, \vec{i} + \sin\theta\, \vec{j},$$

where $\vec{i}$ and $\vec{j}$ are outward pointing unit vectors for the Cartesian system. The z component stresses are

assumed to be negligible: $\tau_{xz} = \tau_{yz} = \sigma_z = 0$. The traction vector acting on ds is then

$$\overset{\upsilon}{T} = \upsilon_j \sigma_{ij} = (\sigma_x \cos\theta + \tau_{xy} \sin\theta)\,\vec{i} + (\sigma_y \sin\theta + \tau_{xy} \cos\theta)\,\vec{j}, \quad (17)$$

where

$$ds = r\, d\theta\, dz. \quad (18)$$

Equation (17) shows that both normal and shear stresses contribute to the traction vector. This means that load and stress measurements that are sensitive only to normal loading will cause structural loads to be underestimated as suggested above. It is also evident that three component stress sensor stations must be used at each measurement site in order to resolve the stress tensor along s.

A calculation using Wang's (1978) solutions will be used to demonstrate the technique and to illustrate the importance of considering shear loads. Wang's solutions are presented in polar coordinates for which, with the aid of a coordinate transformation, Equation (17) takes the form

$$\overset{\upsilon}{T} = (\sigma_r \cos\theta - \tau_{r\theta} \sin\theta)\,\vec{i} + (\sigma_r \sin\theta + \tau_{r\theta} \cos\theta)\,\vec{j}. \quad (19)$$

The force on the cylindrical structure can now be computed for both the fixed and free boundary conditions using Equation (14) and assuming that the direction of loading is co-linear with the x axis (Fig.2)

$$\vec{F} = \int_0^t \int_0^{2\pi} \overset{\upsilon}{T}\, r\, d\theta\, dz. \quad (20)$$

Substituting Equations (1) and (3) in (19) and integrating Equation (20) gives

$$\vec{F} = Pt\pi r/2\,(N_r - N_{r\theta})\,\vec{i} \quad (21)$$

for the fixed boundary condition.

$$F = Ptr/2\,[\underbrace{(1+\nu)/x^3 - (3+\nu)/x}_{\text{radial component}} - \underbrace{((1+\nu)/x^3 + (1-\nu)/x)}_{\text{shear component}}]\,\vec{i} = -2PRt\,\vec{i}$$

and for the frictionless boundary condition

$$F = Ptr/2\,[\underbrace{-((1-\nu)/x^3 + (3+\nu)/x)}_{\text{radial component}} - \underbrace{(-(1-\nu)/x^3\,)1-\nu)/x)}_{\text{shear component}}]\,\vec{i} = 2PRt\,\vec{i}.$$

The relative contribution of the radial and shear components can be shown for the special case where r = R. In this case the force for fixed boundary is

$$F = PtR[\underbrace{-1}_{\text{radial component}} \quad \underbrace{-1}_{\text{shear component}}]\,\vec{i}$$

and for the frictionless boundary

$$F = PtR\,[\underbrace{-2}_{\text{radial component}} \quad \underbrace{-0}_{\text{shear component}}]\,\vec{i}\,.$$

In this example shear stress loading contributes zero to 50% of the total load for the structure depending on the boundary condition. This result demonstrates the importance of including shear force loading measurements in all but the simplest of loading situations (for example, loading perpendicular to one face of a rectangular structure).

In the surface integral formulation $\{\Sigma\}$ is continuous along s. However, in practice $\{\Sigma\}$ will be determined only at a finite number of locations around a structure with Equation (14) to be solved numerically. The accuracy of the surface integral method will thus depend directly on the accuracy of load/stress measurements, the density of measurement locations along s, and the interpolation scheme used in integrating Equation (14) numerically. The density of measurement locations needed to determine structural loading adequately can depend on a number of factors including; the variability of the principal direction of ice movement around a structure, the geometry of the structure, and the size of any independent failure zones across the structure. If measurement sites are too widely spaced, then local effects which may significantly affect the loading could be missed, resulting in inaccurate load estimations.

Two possible deployment schemes for sensors would use the structure geometry to determine s (Fig.2). The first deployment, along s_1, consists of attaching load sensors, sensitive to both normal and shear loading, to a structure around its circumference. A second deployment consists of placing stress sensor arrays (an array is composed of three sensors oriented so that the principal directions can be determined) in the ice along s_2 (Fig.2). Either of the deployment methods can be used to determine the ice loads acting on the region interior to the surface. If grounded ice rubble is in the vicinity of the structure then only the first deployment method will yield reasonable estimates of structural loads. This is because locally grounded ice features can influence the magnitude of load transmitted to a structure (Kry 1978[a]). The effect can be examined by using both of the deployment methods described above. Measurements from the instrumented surface s_1 along the ice/structure interface permit calculation of the ice loading on the structure. A second instrumented surface s_2, enclosing both the structure and rubble field, provides data for calculation of the ice loading on the structure/rubble-field system. The load resistance and stress amplification characteristics of the rubble can then be determined by comparison.

SUMMARY AND CONCLUSIONS

Estimates of ice loads on structures have been obtained by the use of mathematical analyses, small-scale and prototype model tests, and load measurements on full-scale structures. Measurements of ice loads on full-scale structures are needed to provide: (1) data for comparison with the results of the mathematical analyses and scale model tests, (2) lower bound estimates for ice forces, (3) a database of loading events, and (4) a means of examining the influence of grounded ice features on structural ice loads. Methods of obtaining the data include attaching instruments to a structure to measure ice loads, and measuring stress using sensors embedded in the ice around a structure. Mathematical models describing ice/structure interaction are used to interpret

the stress measurements and to calculate ice loads on structures; no method has been described in the literature for interpreting load measurements. The advantage of using a mathematical model for interpreting stress measurements is that only a few sensors are needed to develop an estimate of ice loads on structures. However, the usefulness of the interpretation may be limited by the accuracy of the mathematical description and the uncertainty of using local ice stress measurements to calculate total ice forces.

A method of interpreting load and stress measurements using surface integrals was described in this paper. This uses the concept that the total force acting on a structure can be determined by summing the stress vectors acting on an imaginary surface that encompasses the structure. Application of the surface integral method requires that the normal and shear components of load or stress be known along the surface. This means that sensor arrays, capable of resolving normal and shear loads, must be placed along the surface. The spacing between sensor arrays should be small enough so that local stress or load changes due to the process of ice failure around a structure can be detected. The surface integral method is an attractive technique for interpreting load and stress measurements since a knowledge of the mechanisms of ice/structure interaction is not required. The primary disadvantage of the technique is that a relatively large number of sensors are needed to determine adequately the stress tensor along the surface of interest.

The surface integral method can be used to examine the effects of a grounded rubble field on structural ice loading. One instrumented surface along an ice/structure boundary would be used to determine the load acting on the structure. A second instrumented surface enclosing both the structure and rubble field could then be used to estimate the load acting on the combined structure/rubble-field system.

REFERENCES

APOA 1981 Profile: Ken Croasdale, ice engineer. *A[rctic] P[etroleum] O[perators'] A[ssociation] Review* 4(3): 16-17

Croasdale K R, Morgenstern N R, Nuttall J B 1977 Indentation tests to investigate ice pressures on vertical piers. *Journal of Glaciology* 19(81): 301-312

Danys J V, Bercha F G 1976 Determination of ice forces on a conical offshore structure. *In POAC 75: the third International Conference on Port and Ocean Engineering under Arctic Conditions, Fairbanks, Alaska, 1975. Proceedings Vol 2:* 741-751

Edwards R Y, Croasdale K R 1977 Model experiments to determine ice forces on conical structures. *Journal of Glaciology* 19(81): 660

Kerr A D 1978 On the determination of horizontal forces a floating ice plate exerts on a structure. *Journal of Glaciology* 20(82): 123-134

Kry P R 1978[a] Ice rubble fields in the vicinity of artificial islands. *In POAC 77: the fourth International Conference on Port and Ocean Engineering under Arctic Conditions, St John's, Newfoundland, Canada, 1977. Proceedings Vol 1*: 200-211

Kry P R 1978[b] A statistical prediction of effective ice crushing stresses on wide structures. *In IAHR. International Association for Hydraulic Research. Symposium on ice problems, Luleå, Sweden, 1978. Proceedings Part 1*: 33-47

Kry P R 1980[a] Implications of structure width for design ice forces. *In* Tryde P (*ed*) *International Union of Theoretical and Applied Mechanics. Physics and mechanics of ice. Symposium Copenhagen...1979...* Berlin etc, Springer-Verlag: 179-193

Kry P R 1980[b] Third Canadian Geotechnical Colloquium. Ice forces on wide structures. *Canadian Geotechnical Journal* 17(1): 97-113

Lewis J W, Croasdale K R 1978 Modeling the interaction between pressure ridges and conical shaped structures. *In IAHR. International Association for Hydraulic Research. Symposium on ice problems, Luleå, Sweden, 1978. Proceedings Part 1*: 165-196

Määttänen M 1978 Ice-force measurements at the Gulf of Bothnia by the instrumented Kemi I lighthouse. *In POAC 77: the fourth International Conference on Port and Ocean Engineering under Arctic Conditions, St John's, Newfoundland, Canada, 1977. Proceedings Vol 2*: 730-740

Määttänen M 1980 Ice-force measurements in Finnish lighthouses. *C-CORE Publication* 80-21: 343-353

Metge M, Danielewicz G, Hoare R 1981 On measuring large-scale ice forces; Hans Island 1980. *In POAC 81: the sixth International Conference on Port and Ocean Engineering under Arctic Conditions, Québec, Canada, 1981. Proceedings Vol 2*: 629-642

Neill C R 1971 Ice pressure on bridge piers in Alberta, Canada. *In IAHR. International Association for Hydraulic Research. Symposium on ice and its action on hydraulic structures, Reykjavík, Iceland, 1970.* Paper 6.1

Ralston T D 1978[a] An analysis of ice sheet indentation. *In IAHR. International Association for Hydraulic Research. Symposium on ice problems, Luleå, Sweden, 1978. Proceedings Part 1:* 13-31

Ralston T D 1978[b] Ice force design considerations for conical offshore structures. *In POAC 77: the fourth International Conference on Port and Ocean Engineering under Arctic Conditions, St John's, Newfoundland, Canada, 1977. Proceedings Vol 2:* 741-752

Robbins R J, Verity P H, Taylor T P, Metge M 1976 Techniques for the study of ice-structure interaction. *In POAC 75: the third International Conference on Port and Ocean Engineering under Arctic Conditions, Fairbanks, Alaska, 1975. Proceedings Vol 2*: 911-924

Schwarz J 1971 The pressure of floating ice-fields on piles. *In IAHR. International Association for Hydraulic Research. Symposium on ice and its action on hydraulic structures, Reykjavík, Iceland, 1970.* Paper 6.3

Semeniuk A 1977 Ice pressure measurements at Arnak L-30 and Kannerk G-42. *A[rctic] P[etroleum] O[perators'] A[ssociation] Project* 122

Strilchuk A R 1977 Ice pressure measurements: Netserk F-40, 1975-76. *A[rctic] P[etroleum] O[perators'] A[ssociation] Project* 105

Templeton J S III Unpublished. Ice defense and monitoring. Presented at Technical seminar on Alaska Beaufort Sea gravel island design, presented by Exxon Company, USA, at Anchorage, Alaska, 15 October 1979 and Houston, Texas, 18 October 1979 (Preprint)

Verity P H 1975 A.P.O.A. project 65 small prototype tests, winter 1973/74. *A[rctic] P[etroleum] O[perators'] A[ssociation] Report* 65-1

Wang Y-S 1978 Buckling of a half ice sheet against a cylinder. *Proceedings of the American Society of Civil Engineeers. Journal of the Engineering Mechanics Division* 104(EM5): 1131-1145